Supporting information

Indeno-anthraquinone hosts with thermally activated delayed fluorescence for deep red OLEDs

Ruihuan Liu,[a] Chen Yin,[a] Dongdong Zhang,*[a] and Lian Duan*[ab]

a. Key Lab of Organic Optoelectronics & Molecular Engineering of Ministry of Education, Department of Chemistry, Tsinghua University, Beijing 100084, P. R. China. E-mail: ddzhang@mail.tsinghua.edu.cn, duanl@mail.tsinghua.edu.cn.

b. Center for Flexible Electronics Technology, Tsinghua University, Beijing 10084, P. R. China.

This file includes:

- Synthesis protocol
- TGA, DSC and CV curves
- Supplemental photophysical characterization of IAQ-derivatives in mCP-hosted films with varied doping concentration
- PL transient decay curves of mCP-hosted films at varied temperature.
- Supplemental photophysical characterization of TADF-hosted phosphor films with varied doping concentration
- Current density-voltage curves of single-carrier devices
- Supplemental device performance
- MALDI TOF mass spectra, ^{1}H and ^{13}C NMR spectra

Synthesis pathway

Both IAQ-PhCz and IAQ-CzCz were synthesized via one-step Buchwald-Hartwig reaction between 2-bromo-13,13-dimethyl-6H-indeno[1,2-b]anthracene-6,11(13H)-dione (IAQ-Br) and carbazole derivatives.

- Synthesis of 2-(3,6-diphenyl-9H-carbazol-9-yl)-13,13-dimethyl-6H-indeno[1,2-b]anthracene-6,11(13H)-dione (IAQ-PhCz)

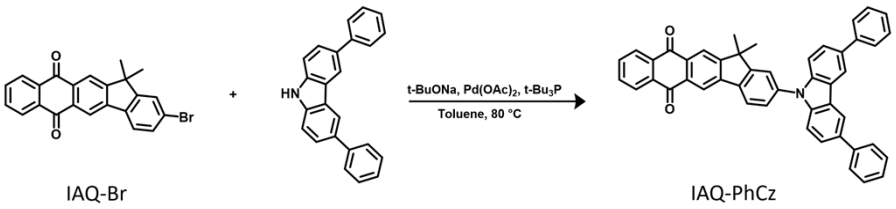

Scheme S1. Synthesis pathway of IAQ-PhCz

3 mmol IAQ-Br (1.21 g), 3.6 mmol 3,6-diphenyl-9H-carbazole (1.15 g), 6 mmol t-BuONa (0.58 g), 0.15 mmol $Pd(OAc)_2$ (0.04 g), 0.45 mmol t-Bu_3P (0.09 g) and 80 ml toluene were added into a two-necked bottle and stirred at 80 °C for 12 hours under nitrogen protection. Then the reaction was cooled to room temperature and quenched by 100 ml water. Extraction by dichloromethane (DCM) was operated for three times. The organic layer was combined and dried with anhydrous Na_2SO_4, followed by solvent removal under reduced pressure for crude product. Further purification was

carried out by silica column chromatography using a petroleum ether/DCM of 4:1 as solvent. Final product was obtained as an orange solid (1.12 g, 62%). ^{1}H NMR (DMSO-D_6):δ 8.75 (m, 3H), 8.46 (d, 1H), 8.44 (s, 1H), 8.24 (m, 2H), 8.07 (d, 1H), 7.93 (m, 2H), 7.80 (m, 6H), 7.74 (d, 1H), 7.54 (d, 2H), 7.48 (t, 4H), 7.34 (t, 2H), 1.64 (s, 6H). MALDI m/z: 641 $[M]^+$.

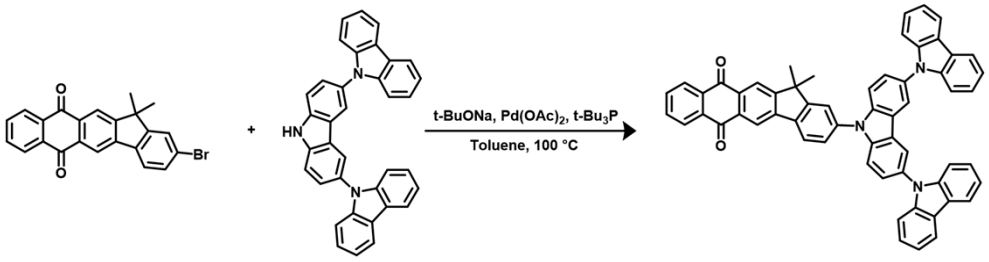

Scheme S2. Synthesis pathway of IAQ-CzCz

3 mmol IAQ-Br (1.21 g), 4 mmol 9'H-9,3':6',9''-tercarbazole (1.99 g), 8 mmol t-BuONa (0.77 g), 0.2 mmol $Pd(OAc)_2$ (0.05 g), 0.6 mmol t-Bu_3P (0.12 g) and 80 ml toluene were added into a two-necked bottle and stirred at 100 °C for 12 hours under nitrogen protection. Then the reaction was cooled to room temperature and quenched by 100 ml water. Extraction by dichloromethane (DCM) was operated for three times. The organic layer was combined and dried with anhydrous Na_2SO_4, followed by solvent removal under reduced pressure for crude product. Further purification was carried out by silica column chromatography using a petroleum ether/DCM of 3:1 as solvent. Final product was obtained as an orange solid (1.11 g, 45%). ^{1}H NMR (DMSO-D_6):δ 8.81 (s, 1H), 8.69 (d, 2H), 8.55 (d, 1H), 8.47 (s, 1H), 8.24 (m, 7H), 7.93 (m, 3H), 7.77 (d, 2H), 7.68 (m, 2H), 7.38 (m, 8H), 7.25 (m, 4H), 1.69 (s, 6H). MALDI m/z: 820 $[MH]^+$.

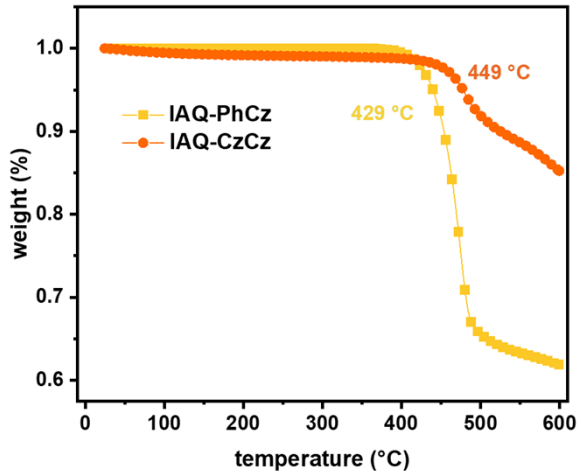

Fig. S1. Thermogravimetric analysis (TGA) curves of IAQ-PhCz and IAQ-CzCz.

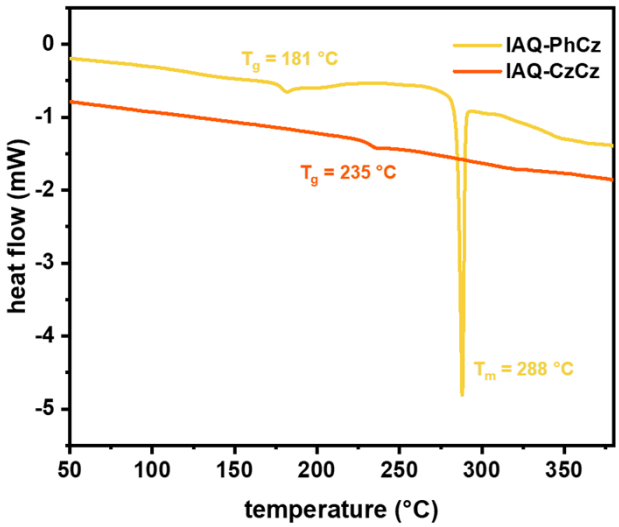

Fig. S2. Differential scanning calorimetry (DSC) curves of IAQ-PhCz and IAQ-CzCz.

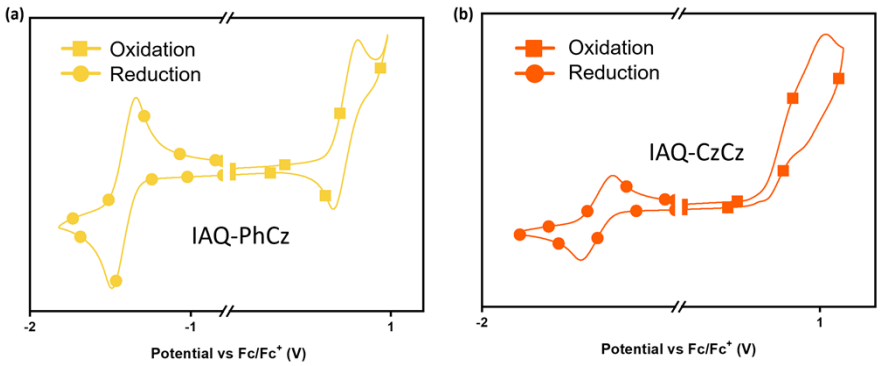

Fig. S3. Cyclic voltammetry curves of (a) IAQ-PhCz and (b)IAQ-CzCz.

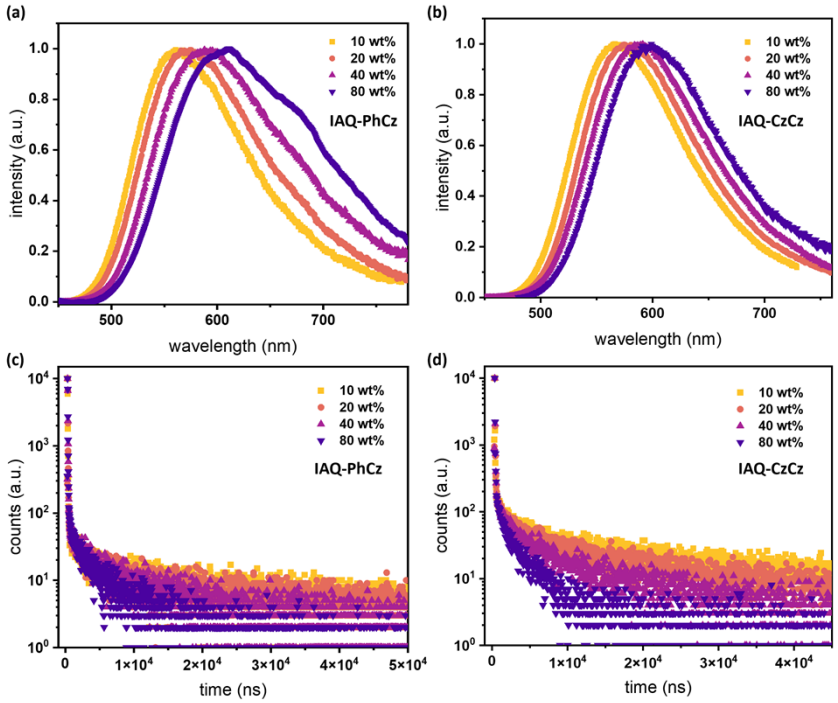

Fig. S4. Photophysical properties of IAQ-PhCz and IAQ-CzCz doped in mCP films with varied doping concentration. (a) PL spectra and (b)transient decay curves of IAQ-PhCz doped mCP films measured at room temperature under ambient atmosphere. (c) PL spectra and (d) transient decay curves of IAQ-CzCz doped mCP films.

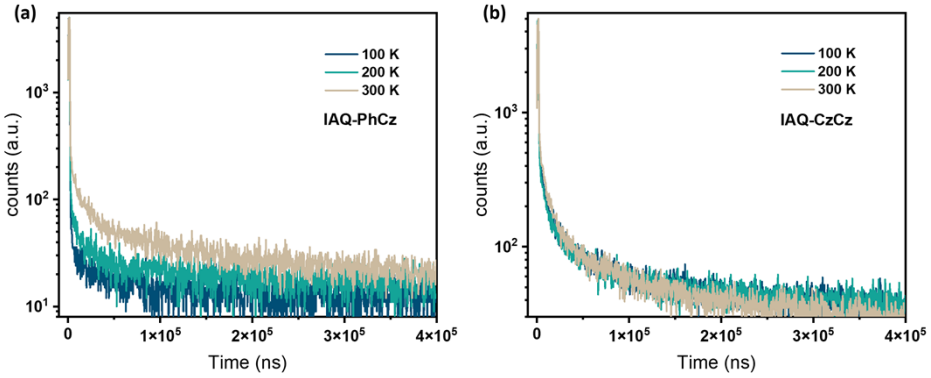

Fig. S5. Transient decay curves of (a) IAQ-PhCz and (b) IAQ-CzCz mCP-hosted films (10 wt%) at varied temperatures under vacuum.

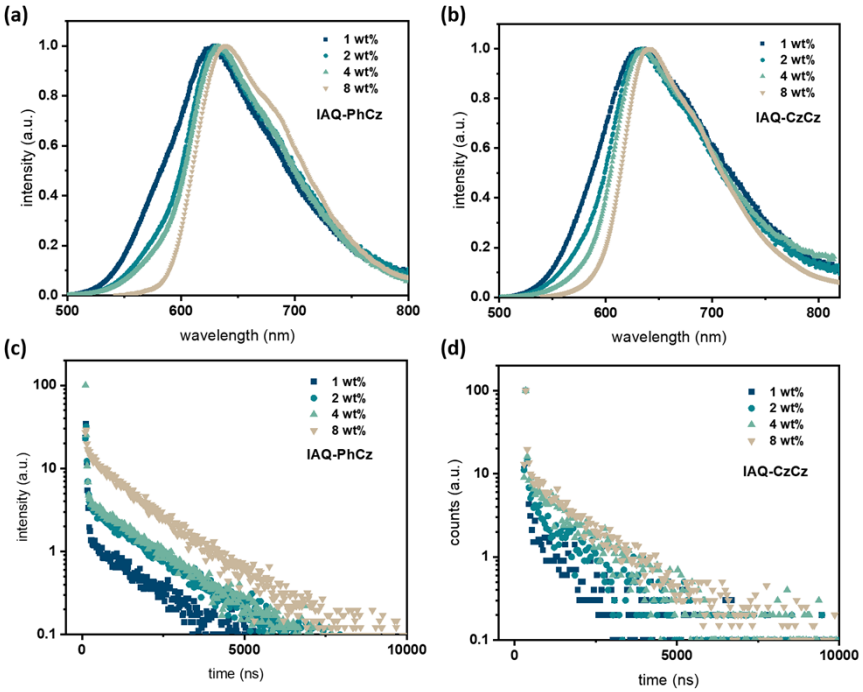

Fig. S6. Photophysical characterization of TADF-hosted phosphor films with varied phosphor doping under ambient condition. PL spectra of (a) IAQ-PhCz-hosted and (b) IAQ-CzCz-hosted films. PL transient decay curves of (c) IAQ-PhCz-hosted and (d) IAQ-CzCz-hosted films.

Table S1. Summary of PLQY values of IAQ-PhCz- and IAQ-CzCz-hosted films with varied phosphor doping.

Ir-doping	IAQ-PhCz	IAQ-CzCz
1 wt%	0.27	0.31
2 wt%	0.38	0.43
4 wt%	0.43	0.54
8 wt%	0.62	0.74

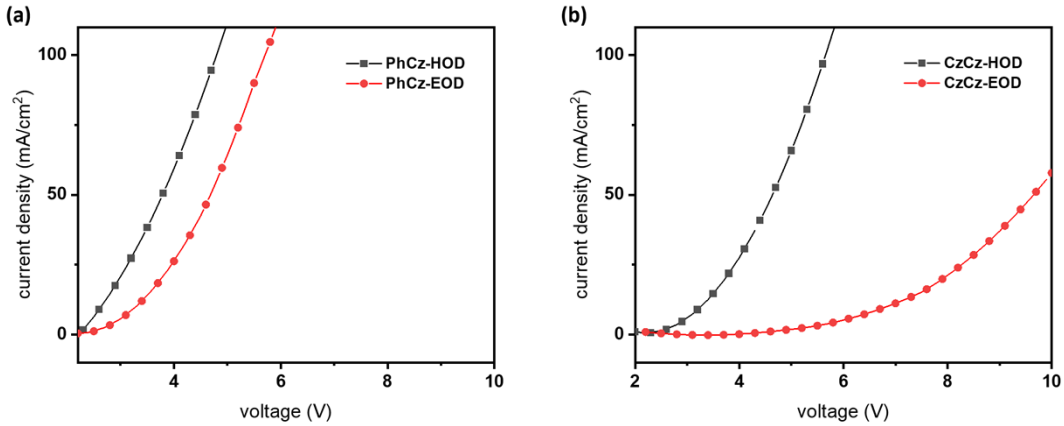

Fig. S7. The current density-voltage curves of hole-only-device (HOD) and electron-only-device (EOD) of (a) IAQ-PhCz and (b) IAQ-CzCz.

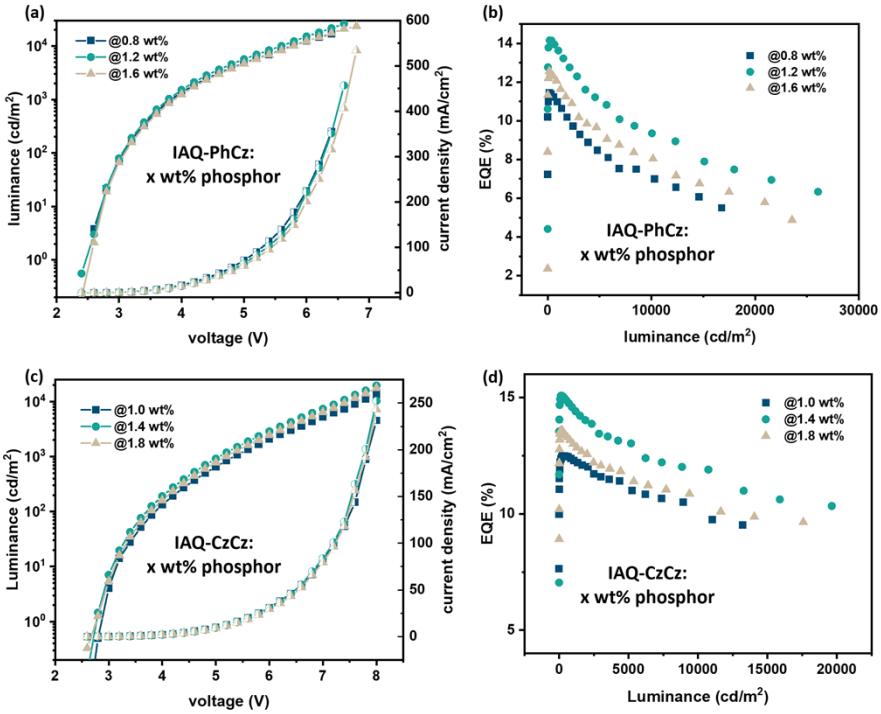

Fig. S8. Device performances of TSP devices with varied doping of phosphor. (a) Luminance-voltage-current density (L-V-J) curves and (b) EQE-luminance curves of IAQ-PhCz based TSP devices with varied phosphor doping; (c) L-V-J and (d) EQE-L curves of IAQ-CzCz based TSP devices with different phosphor doping.

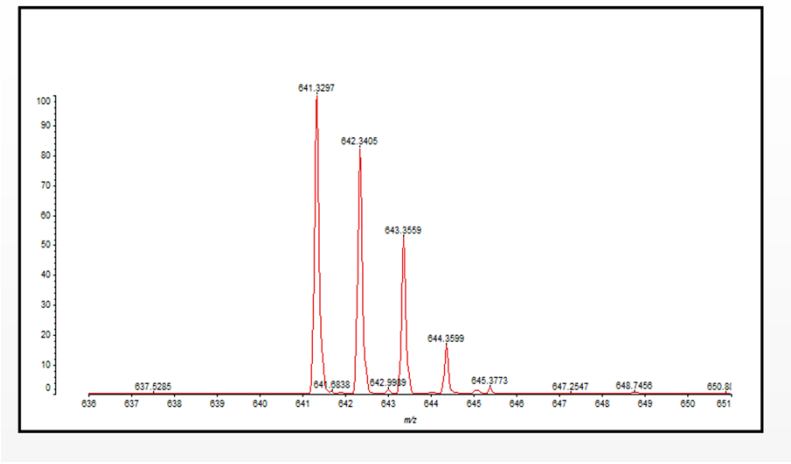

Fig. S9. MALDI-TOF mass spectra of IAQ-PhCz.

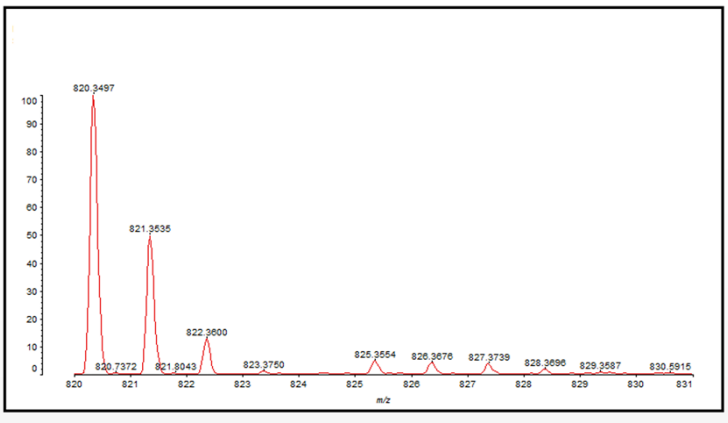

Fig. S10. MALDI-TOF mass spectra of IAQ-CzCz.

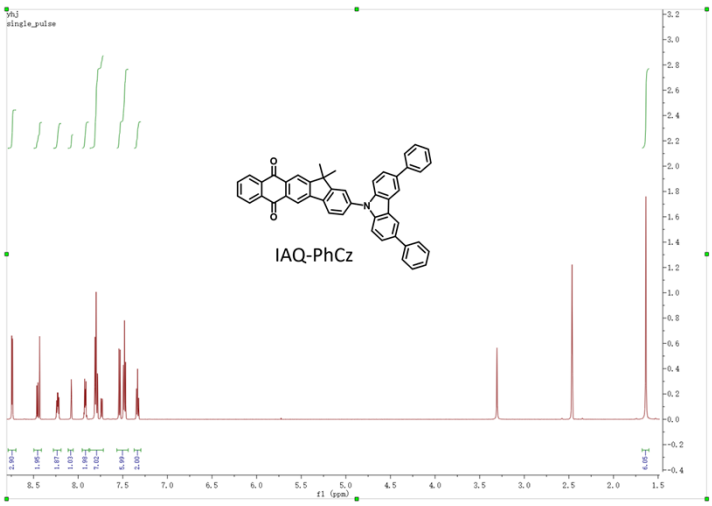

Fig. S11. ^{1}H NMR spectrum of IAQ-PhCz (DMSO-D_6).

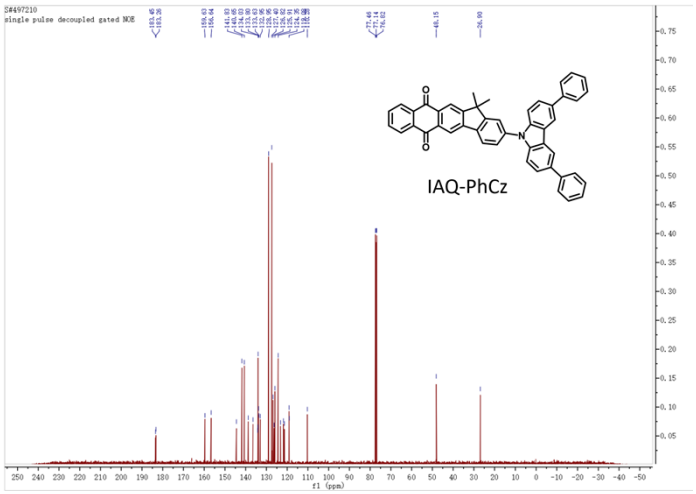

Fig. S12. ^{13}C NMR spectrum of IAQ-PhCz ($CDCl_3$).

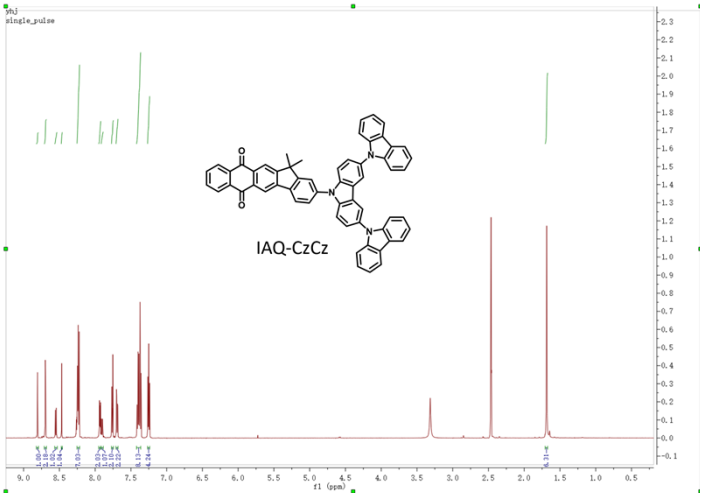

Fig. S13. ^{1}H NMR spectrum of IAQ-CzCz (DMSO-D_6).

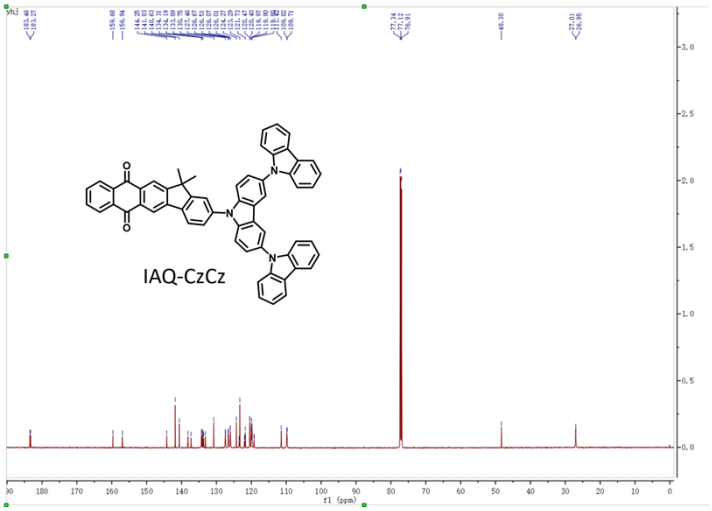

Fig. S14. ^{13}C NMR spectrum of IAQ-CzCz ($CDCl_3$).